J. Fluid Mech. (2013), *vol.* 715, *pp.* 452–476. © Cambridge University Press 2013
doi:10.1017/jfm.2012.529

Shear instability as a resonance between neutral waves hidden in a shear flow

Keita Iga†

Atmosphere and Ocean Research Institute, The University of Tokyo, Kashiwa, Chiba 277-8564, Japan

(Received 21 December 2010; revised 25 September 2012; accepted 23 October 2012)

A concept which explains unstable modes by resonance between two neutral waves is applied to instability in shear flows with non-uniform potential vorticity distribution. In basic flows where shear instability occurs, a pair of neutral waves which should resonate to form an unstable mode does not exist mathematically unless the basic potential vorticity is uniform, owing to the shear of the basic flow. However, if a small window region is made where the potential vorticity of the basic flow is uniform, regular neutral modes can exist. The neutral wave located at the centre of this window region, which corresponds to a mode where the jump in its first derivative at one end of the window region cancels that at the other end, can be considered to be the hidden neutral wave. It is equivalent to a continuous mode which does not have a jump in its first derivative at the critical point even though it can have a singularity of $(y - y_c) \log |y - y_c|$, in the limit of an infinitely small window region. Thus, a method for retrieving neutral waves hidden in the shear of the basic flow is proposed here. By sweeping the basic flow range with this uniform potential vorticity window, all the features of the hidden neutral wave appear. By applying this method, shear instability in a flow with a tanh-shaped basic velocity profile is well explained via the resonance between neutral waves.

Key words: critical layers, shear layers, shear waves

1. Introduction

In fluid dynamics, including dynamical meteorology and physical oceanography, instability of parallel flows is an important problem, and many situations have been investigated. The linear instability problems are mathematically established as eigenvalue problems, and thus it is not difficult to obtain the solutions, but the results obtained are often too complicated to understand physically.

Explanation of unstable modes via resonance between neutral waves is often useful for understanding physically such complicated unstable modes (Cairns 1979). The most direct application of this concept is to analyse 'subsystems' of the whole system. First, we investigate the neutral waves in each subsystem. When the phase speed of a certain wave in a subsystem coincides with that in another, the waves that exist as neutral waves in the subsystems sometimes resonate, causing instability in the whole system. By decomposing the unstable mode into neutral waves in the subsystems, understanding of its features becomes easier. Using this concept, Sakai (1989),

† Email address for correspondence: iga@aori.u-tokyo.ac.jp

https://doi.org/10.1017/jfm.2012.529 Published online by Cambridge University Press

Iga (1993, 1997) and Iga & Ikazaki (2000), for example, clearly classified complicated unstable modes which appear in two-layer problems.

In some instability problems, however, we cannot easily construct subsystems. Even in such situations, we can identify the neutral waves in the full system which resonate to cause the instability, by finding two dispersion curves of neutral modes leading to that of the unstable mode, as shown by Hayashi & Young (1987).

The above examples are all explained by resonance between the usual regular modes. However, the shear of the basic flow definitely affects the existence of neutral modes. According to Lin's theorem (Lin 1945), a regular neutral mode with a critical point ($y = y_c$), where the phase speed c coincides with the velocity of the basic flow ($U(y_c) = c$), can exist only when the potential vorticity gradient vanishes there ($Q'(y_c) = 0$). In fact, the above examples are all categorized into special cases where either velocity or potential vorticity is uniform. In general, it is impossible to find neutral modes.

Critical layer instability (Bretherton 1966) is an example of such instabilities wherein a pair of neutral modes cannot easily be found, but explanation of critical layer instability via resonance between neutral waves is shown by Iga (1999*a*). In this case, continuous modes with singularity at the critical point, which exist when the basic flow has a shear (Case 1960), play an important role. (We will call singular modes consisting of a continuous spectrum 'continuous modes'.) Iga (1999*a*) showed that critical layer instability can be understood via resonance between neutral waves if we consider a usual regular mode as one counterpart of the resonating pair and a bundle of continuous modes with singularities as the other.

Nevertheless, some instabilities are still not explained even if we include a continuous spectrum (a bundle of continuous modes) as a candidate for the resonating neutral waves. We cannot apply the analysis method mentioned above to shear instability in a basic flow with a tanh-shaped velocity profile, which is one of the simplest instability problems, as will be discussed in the next section. It is known that shear instability in some situations is understood via resonance between neutral waves. The idea is extended to more general cases by Baines & Mitsudera (1994). However, the calculation is applicable only when the potential vorticity around the critical point is uniform. The identification of neutral modes is achieved relatively easily inside the region where the potential vorticity is uniform, but it is not straightforward when the potential gradient is not zero. In this paper, we intend to establish a more general analysis approach to instability via resonance between neutral waves, by making this method applicable also to instabilities in such shear flows.

In basic flows with smooth velocity profiles, such as a tanh-shaped flow, if the growth rate of an unstable mode decreases as the wavenumber increases, finally becoming zero at a certain wavenumber, we cannot investigate the continuing modes with a larger wavenumber in a simple way because of the mathematical difficulty of critical points, and this is the origin of the essential problem considered here. We can proceed with discussion of this problem by considering features of continuous modes. However, there is another way to investigate how the unstable modes are extended to a large-wavenumber region: considering small but non-zero viscosity, we can discuss the modes as the inviscid limit of viscous flows. In fact, similar problems were studied according to this approach in the 1960s (e.g. Tatsumi, Gotoh & Ayukawa 1964; Gotoh 1965), and are now given in textbooks (e.g. Drazin & Reid 1981). In general, a mode in an inviscid flow is not the same as one in the inviscid limit of viscous flows unless it is a growing mode with phase speed having positive imaginary part. When considering the inviscid limit of viscous flows, the mode in a large-wavenumber region

https://doi.org/10.1017/jfm.2012.529 Published online by Cambridge University Press

is a decaying mode with finite decay rate even at the zero limit of viscosity; the mode has a singularity in this limit and is influenced by viscosity even when the viscosity coefficient becomes infinitely small. According to the different effects of viscosity, these two methods derive different modes in a large-wavenumber region connecting to an unstable mode. This means that the two approaches provide two different means of decomposing small-scale disturbances which consist mainly of large-wavenumber modes, since considering modes is a means of decomposing disturbances.

Since there are two different approaches, we need to choose the more appropriate way to describe phenomena. In general descriptions of fluid phenomena, the classical way to consider inviscid limit of viscous flows often has the advantage that it is easy to compare the results directly with the phenomena since real fluid has non-zero viscosity. However, the problem treated in this study is understanding unstable modes via resonance between neutral waves, and this concept, which has been applied since the 1970s, is based on conservation of pseudomomentum (or pseudoenergy) in inviscid flows. Therefore, the method of considering the inviscid limit of viscous flows, where the modes are directly influenced by viscosity and thus have finite decay rates even in the inviscid limit, cannot be easily applied, at least to the present problem. We will adopt the method of using continuous modes in this study, to which we can apply this concept based on the conservation of pseudomomentum in a more straightforward way.

Tatsumi *et al.* (1964) also calculate the dispersion relation of the broken-line velocity profile case where the potential vorticity is piecewise uniform. We must check the consistency of their results with the discussions in this article.

This paper is organized as follows. In § 2, we will show a problem which arises when applying the concept of resonance between neutral waves to shear instability. In § 3, we will explain the method of 'opening a window in the basic flow', which removes this difficulty. The essence of this method will be described in the context of continuity of eigenfunctions in § 4, and in relation to continuous modes in § 5. We will apply this established method to the shear flow with a tanh-shaped profile and show the numerical result in § 6. In § 7, we will also solve the broken-line velocity profile case, and explain the relationship with the present case. Finally, conclusions are given in § 8.

2. Neutral waves leading to the shear instability mode

We will consider disturbances in parallel flows of two-dimensional fluid spreading infinitely with constant density ρ_0 in a rotating frame with Coriolis parameter $f = f_0 + \beta y$:

$$\frac{\partial u'}{\partial t} + U\frac{\partial u'}{\partial x} + v'\frac{\mathrm{d}U}{\mathrm{d}y} - fv' = -\frac{1}{\rho_0}\frac{\partial p'}{\partial x}, \tag{2.1}$$

$$\frac{\partial v'}{\partial t} + U\frac{\partial v'}{\partial x} + fu' = -\frac{1}{\rho_0}\frac{\partial p'}{\partial y}, \tag{2.2}$$

$$\frac{\partial u'}{\partial x} + \frac{\partial v'}{\partial y} = 0, \tag{2.3}$$

where u' and v' denote the disturbance velocities in the x- and y-directions, p' is the disturbance pressure, and U, the basic velocity in the x-direction, is a function of y. Introducing stream function ϕ defined by $u' = -\partial\phi/\partial y$, $v' = \partial\phi/\partial x$, and considering

https://doi.org/10.1017/jfm.2012.529 Published online by Cambridge University Press

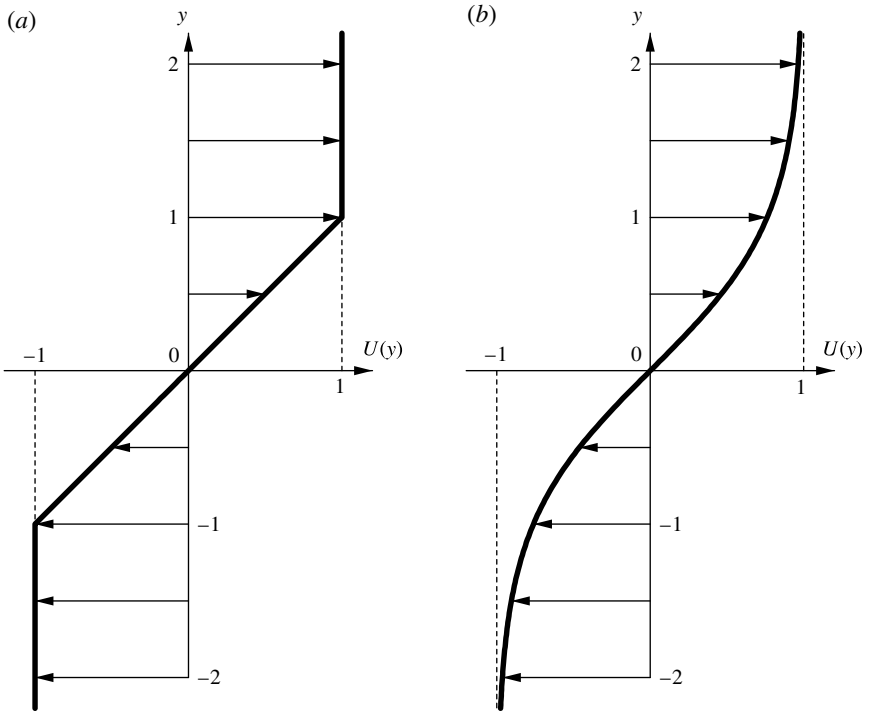


FIGURE 1. Two basic shear flows considered in this article. (*a*) A case where the $U(y)$ profile is piecewise linear: $U(y) = -1$ at $y < -1$, $U(y) = y$ at $-1 < y < 1$, and $U(y) = 1$ at $y > 1$. (*b*) A case with a tanh-shaped profile $U(y)$: $U(y) = \tanh y$.

sinusoidal wave disturbances in the form $\exp[\mathrm{i}k(x - ct)]$, the basic equation becomes

$$(U - c)\left(\frac{\mathrm{d}^2\phi}{\mathrm{d}y^2} - k^2\phi\right) + \frac{\mathrm{d}Q}{\mathrm{d}y}\phi = 0, \tag{2.4}$$

where $Q \equiv f - \mathrm{d}U/\mathrm{d}y$, and thus $\mathrm{d}Q/\mathrm{d}y = \beta - \mathrm{d}^2U/\mathrm{d}y^2$. In this article, we only consider the case of $\beta = 0$. In some situations, Q may have discontinuity. In this case, we can apply the connection condition across the discontinuity point y_d: $(U - c)\mathrm{d}\phi/\mathrm{d}y + Q\phi$ is continuous across y_d.

Let us consider here two cases with similar basic flow profiles $U(y)$ as shown in figure 1. One is a case where the $U(y)$ profile is piecewise linear: $U(y) = -1$ at $y < -1$, $U(y) = y$ at $-1 < y < 1$, and $U(y) = 1$ at $y > 1$. The other is a case with a smooth tanh-shaped profile $U(y)$: $U(y) = \tanh y$. Each case represents a simple model of a shear flow where the velocity difference and the width of the shear zone are both unity.

For the first case (figure 1*a*), the problem is analytically solved without difficulty (e.g. Vallis 2006). The phase speed c of the regular mode is solved as a function of the wavenumber k,

$$c = \pm\frac{\sqrt{(1 - 2k)^2 - \mathrm{e}^{-4k}}}{2k}, \tag{2.5}$$

https://doi.org/10.1017/jfm.2012.529 Published online by Cambridge University Press

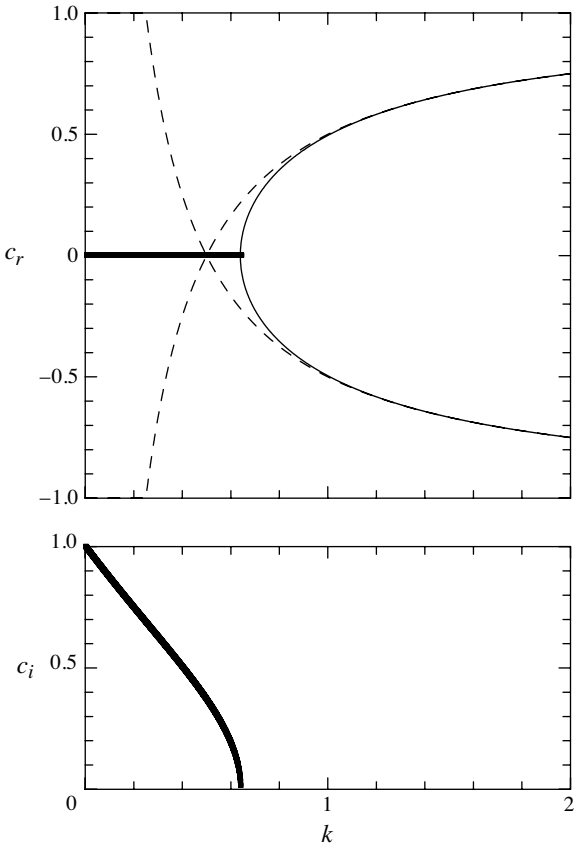


FIGURE 2. Dispersion curves for piecewise linear basic flow case (figure 1*a*). An unstable mode exists at $k < k_c$ and two neutral waves at $k > k_c$, where the value of the critical wavenumber is about $k_c \sim 0.6392$. The dispersion curves of these two neutral waves coalesce, and are connected to that of the unstable mode at $k = k_c$. The dashed lines indicate dispersion curves for the neutral waves in the subsystems (figure 3).

which indicates that an unstable mode and a decaying mode exist at $k < k_c$, and that two neutral modes exist at $k > k_c$, where k_c is the critical wavenumber whose value is $k_c \sim 0.6392$. We can see in figure 2 that the dispersion curve of an unstable mode, which lies on $c_r = 0$ at $k < k_c$, is connected to two dispersion curves of neutral modes. We can construct subsystems without difficulty in this case, and thus we can understand this instability as resonance between neutral waves by investigating the neutral waves in these subsystems. We can consider two settings with only one cusp in the basic velocity distribution as subsystems: (i) $U(y) = y$ at $y < 1$, and $U(y) = 1$ at $y > 1$ (figure 3*a*), and (ii) $U(y) = -1$ at $y < -1$ and $U(y) = y$ at $y > -1$ (figure 3*b*). We investigate the dispersion curves and the eigenfunctions of the waves there, and compare them with those of the unstable mode in the original setting. In figure 2, these dispersion curves are also shown by dashed lines: we can see that the unstable mode exists around the crossing of the dispersion curves of the neutral waves in the subsystems. Further, as shown in figure 4(*a–c*), we can reconstruct the structure of the unstable mode by shifting the eigenfunctions of the neutral modes in the x-direction

https://doi.org/10.1017/jfm.2012.529 Published online by Cambridge University Press

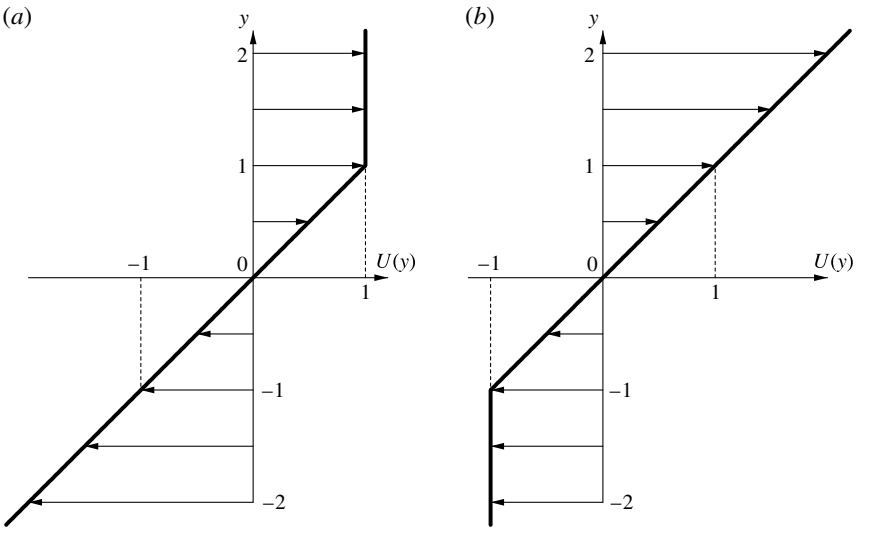


FIGURE 3. Two subsystems of the piecewise linear basic flow (figure 1*a*). (*a*) A basic flow $U(y) = y$ at $y < 1$ and $U(y) = 1$ at $y > 1$: the waves are trapped at $y = 1$ in this system. (*b*) A basic flow $U(y) = -1$ at $y < -1$ and $U(y) = y$ at $y > -1$: the waves are trapped at $y = -1$ in this system.

and superposing them: it suggests that this instability can be recognized as 'interaction' or 'resonance' between the neutral waves.

In this case, we can also apply the method to investigate the pair of neutral waves whose dispersion curves are connected to that of the unstable mode; this method is applicable even to cases where we cannot easily construct subsystems. Comparing the structure of the eigenfunction of the unstable mode with those of the connecting neutral modes (figure 4*a*,*d*,*e*), we can reconstruct the structure of the unstable mode by elongating and shifting the eigenfunctions of the neutral modes in the x-direction and superposing them.

On the other hand, in the shear instability problem for the basic flow profile $U(y) = \tanh y$ (figure 1*b*), it is known that there exists an unstable mode at the wavenumber region $k < 1$ (Michalke 1964). However, since this basic flow profile satisfies $Q'(y) < 0$ at $y < 0$ and $Q'(y) > 0$ at $y > 0$, by Lin's theorem (Lin 1945) the neutral waves with non-zero phase speed do not exist: an unstable mode at $k < 1$ and a neutral mode at $k = 1$ are the only regular modes in this problem. Thus, we cannot find neutral waves which lead to the unstable mode (figure 5*a*). Since the basic flow has a shear, however, continuous modes with singularity at the critical point exist (Case 1960) over the basic flow velocity range (figure 5*b*).

Figure 6 shows the dispersion relation of this problem which is obtained numerically by finite difference; it shows, besides the unstable mode at $k < 1$, discretized continuous modes inside the range $-1 < c < 1$. In the case of a critical layer instability, where only one regular mode exists leading to the unstable mode, we can understand the instability as resonance between neutral waves, by considering the bundle of the continuous modes as a counterpart of the resonating pair (Iga 1999*a*). By analogy, an idea may arise that the shear instability whose dispersion curve leads to no neutral mode might be considered to be a resonance between two bundles of continuous modes. In fact, the dispersion curves obtained by the discretized calculation

https://doi.org/10.1017/jfm.2012.529 Published online by Cambridge University Press

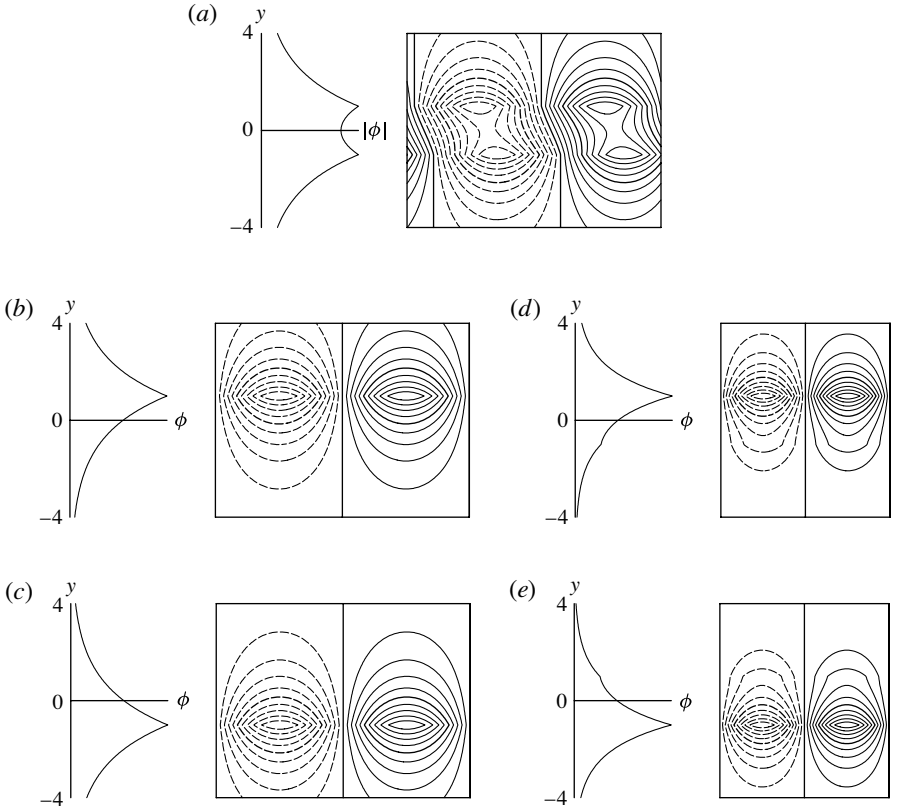


FIGURE 4. (*a*) Unstable mode at $k = 0.6$ for the basic flow of figure 1(*a*) ($c = 0.1877\mathrm{i}$). (*b*) Neutral mode at $k = 0.6$ for the subsystems of figure 3(*a*) ($c = -0.1667$). (*c*) Neutral mode at $k = 0.6$ for the subsystems of figure 3(*b*) ($c = 0.1667$). (*d*) Neutral mode with positive phase speed $c = 0.4349 > 0$ at $k = 0.9$ for the basic flow of figure 1(*a*). (*e*) Neutral mode with negative phase speed $c = -0.4349 < 0$ at $k = 0.9$ for the basic flow of figure 1(*a*). The neutral waves (*b*) and (*c*) have an amplitude peak around $y = 1$ and $y = -1$, respectively. The structure of the unstable mode is similar to the superposition of structures of the two neutral waves shifted in the *x*-direction; it shows that the unstable mode can be explained via resonance between these neutral waves. The structure of the unstable mode is also similar to the superposition of structures of two neutral waves (*d*) and (*e*) elongated and shifted in the *x*-direction.

show that two or three of the discretized dispersion curves seem to coalesce to make the unstable mode (figure 6). However, this explanation has a serious difficulty. Continuous modes which lead to the unstable mode when discretized are neighbouring continuous modes, which converge to the same mode with $c = 0$ in the limit of infinitely small finite-difference interval. Although we intend to find a resonating pair, these modes become identical. We cannot help but consider modes other than these continuous modes as the resonating pair.

The most serious problem in finding a resonating pair of neutral waves other than continuous modes is that we cannot obtain any regular modes as mathematical solutions. Let us consider this problem in detail. If there existed a pair of neutral waves connected to the unstable mode, one would appear as a mode starting from

https://doi.org/10.1017/jfm.2012.529 Published online by Cambridge University Press

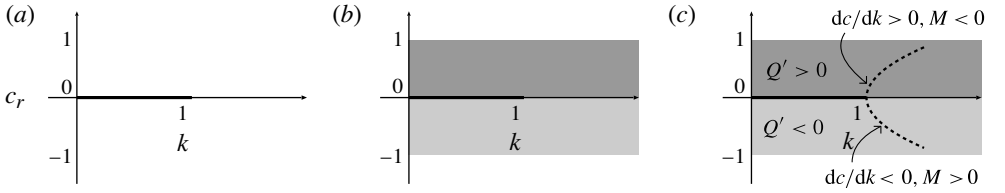


FIGURE 5. (*a*) A schematic view of the dispersion relation of the regular mode in the basic flow $U = \tanh y$. An unstable mode with $c_r = 0$ exists only in the wavenumber $0 < k < 1$, and no regular mode in $k > 1$. (*b*) Continuous modes besides the regular mode are also shown. All over the region $-1 < c_r < 1$ there exist continuous modes. (*c*) Expected dispersion curves at $k > 1$ leading to the unstable mode. The branch with $c_r > 0$ should have negative pseudomomentum since it satisfies $\mathrm{d}c/\mathrm{d}k > 0$. In this phase speed range, the basic flow has $\mathrm{d}Q/\mathrm{d}y > 0$ at the point where the basic flow velocity coincides with this phase speed. On the other hand, on the branch with $c_r < 0$, the pseudomomentum must be positive, and the basic flow has $\mathrm{d}Q/\mathrm{d}y < 0$.

$k = 1, c = 0$ and entering the region $k > 1, c > 0$, and the other as a mode starting from the same point and entering the region $k > 1, c < 0$ (figure 5*c*). The former would have a positive gradient of the dispersion curve in the k–c plane ($\mathrm{d}c/\mathrm{d}k > 0$), and Iga (1999*b*) showed that a mode with $\mathrm{d}c/\mathrm{d}k > 0$ has a negative pseudomomentum. Moreover, inside this region of $c > 0$, there exists a critical point y_c where the velocity of the basic flow U coincides with the phase speed, and it satisfies $Q'(y_c) > 0$. When a wave mode with negative pseudomomentum enters a basic flow range, the behaviour of the wave affected by the basic flow depends on the sign of the potential vorticity gradient at the critical point $Q'(y_c)$: the wave mode becomes an unstable mode if $Q'(y_c) < 0$, while the regular mode disappears within the basic flow if $Q'(y_c) > 0$ (Iga 1999*a*). Therefore, such a mode with $k > 1, c > 0$, if it existed physically, would disappear in the range of basic shear flow. In the same way the mode for $c < 0$ also disappears, and, indeed, no neutral waves leading to the unstable mode exist in this problem.

From the considerations above, we may come up with an idea as follows. Although resonating neutral waves exist physically, they do not appear as mathematical solutions since they are hidden in the basic flow. Shear instability may be explained by a resonance between such neutral waves hidden in the basic flow. In order to justify this idea, however, we must retrieve the hidden neutral waves by other means.

3. A method for retrieving hidden neutral waves

Even though it may be physically plausible to think that a neutral wave exists, it does not mathematically. So how should we understand it? Lin's theorem insists that within the velocity range of the basic flow, a neutral wave with the corresponding phase speed does not exist (except the case when the potential vorticity gradient just vanishes there). It may be possible to understand it as follows. Even if there seems to exist a neutral wave inside the range of the basic flow velocity, the basic flow acts as a kind of 'barrier' which obstructs the existence of the neutral wave. Then, we may be able to retrieve the hidden neutral wave by removing the barrier.

The next question is how we remove the barrier. Considering the condition for neutral waves to exist shown by Lin's theorem, we have two approaches. One is to modify the basic flow to one with a piecewise uniform velocity profile so that the

https://doi.org/10.1017/jfm.2012.529 Published online by Cambridge University Press

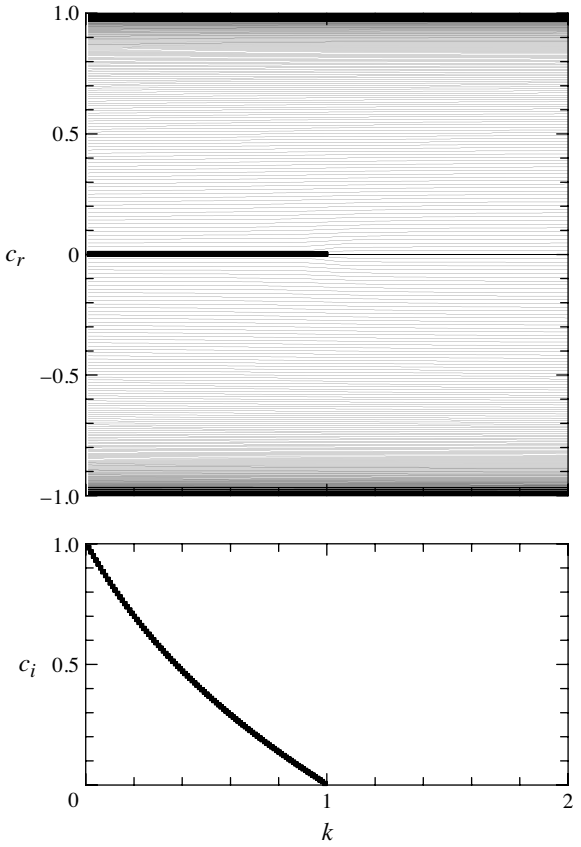


FIGURE 6. Numerically solved dispersion relation for the tanh-shaped velocity profile basic state. The region $-8 < y < 8$ is finite-differenced with 1000 grid points. An unstable mode, which is shown by a thick line, is located at $k < 1$. Neutral modes shown by thin lines are all discretized continuous modes.

distribution of the basic flow velocity is confined to several values only. The other, noticing the exceptional case wherein neutral waves with a critical point can exist, is to modify the basic flow so that its potential vorticity profile becomes piecewise uniform. Taniguchi & Ishiwatari (2006) applied the first method to a shallow-water shear flow on an equatorial beta plane. In general, however, the velocity profile of the basic flow constructed in this way has many jumps, which may cause unintended instability. In the latter case, there is less possibility of causing such instability, since the velocity profile itself does not have jumps although the potential vorticity profile does. Therefore, we will proceed using the latter method here.

Even if we can remove the barrier by modifying the basic flow profile into that with piecewise uniform potential vorticity distribution, there still remains a problem. The propagation mechanism of many waves crucially depends on potential vorticity distribution. Hence, drastic modification of the potential vorticity distribution will change the propagation characteristics of the targeted neutral wave. In the shear flow with a tanh-shaped velocity profile, for example, neutral waves do not appear if we make the potential vorticity completely uniform. In order to see a wave hidden behind a barrier, one must remove the barrier, but this operation itself affects the existence of

https://doi.org/10.1017/jfm.2012.529 Published online by Cambridge University Press

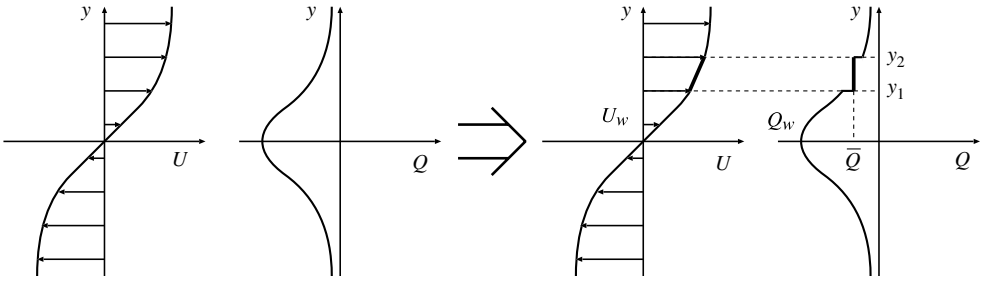


FIGURE 7. A method to open a small window region in the basic state. We make the velocity profile of the basic state linear, or make the potential vorticity profile uniform, only in a very small region $y_1 < y < y_2$; with this modification, neutral waves can exist inside this window region.

the neutral wave: the retrieved wave may be different from the original one or even disappear in some cases.

In order to solve this problem, we will apply the following method. It is because we try to obtain perfect perspective at once by removing the whole barrier that the features of the wave behind the barrier are substantially changed. Accordingly, instead of removing the whole barrier, let us open a small 'observation window' or 'slit' in the barrier which has only a little influence on the hidden wave (figure 7). We can expect the influence to be small enough by making the window opening sufficiently narrow. In order to minimize the modification of the situation, we keep the original velocity profile of the basic state U except the window region $y_1 < y < y_2$. In the case of $\beta = 0$, the uniform potential vorticity distribution in the range of $y_1 < y < y_2$ is realized by changing the profile into the linear velocity profile connecting the velocities $U(y_1)$ at y_1 and $U(y_2)$ at y_2,

$$U_w(y) = U(y_1) + \frac{U(y_2) - U(y_1)}{y_2 - y_1}(y - y_1), \tag{3.1}$$

where the subscript 'w' indicates a modified basic state and the corresponding solutions. The potential vorticity $Q_w(y)$ inside this small window region has a constant value $\overline{Q}$ which, from (3.1), satisfies

$$\overline{Q} = \frac{1}{y_2 - y_1}\int_{y_1}^{y_2} Q(y)\,\mathrm{d}y. \tag{3.2}$$

Naturally, the features of the hidden neutral wave which we can see in this way are only a very small part. However, repeating this operation, sweeping all the parts of the barrier and integrating the obtained results will show us the whole image of the hidden wave. An actual execution of this retrieval of hidden neutral waves by opening a small window on the barrier caused a problem to come to the fore. The dispersion relation of a neutral wave which appears in the window region (figure 8) shows that a neutral wave exists for any value of wavenumber. This phenomenon always occurs wherever the small window region is opened. Figure 9, which shows the eigenfunctions of the waves, indicates that when the phase speed of the mode is close to one end of the window region, the eigenfunction is strongly modified there. In order to extract modes which are less influenced by the ends of the window region, we will search for neutral waves whose phase speed is located at the centre of the window region.

https://doi.org/10.1017/jfm.2012.529 Published online by Cambridge University Press

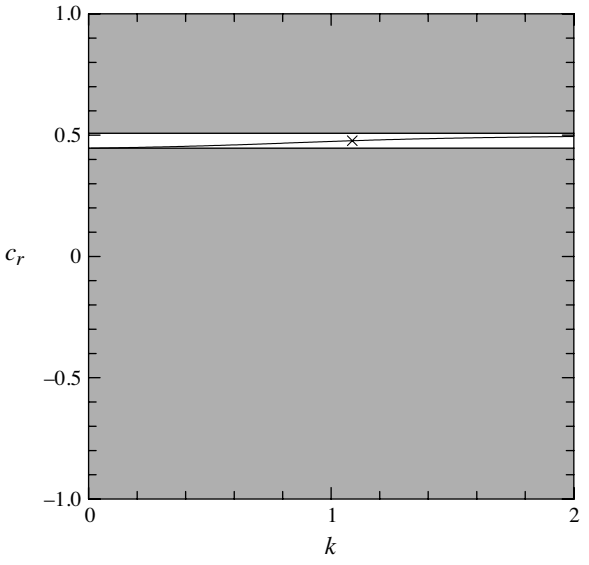


FIGURE 8. A numerically obtained dispersion curve of a regular mode which appears in a window region. For the numerical calculation, 1000 grid points are placed in the region $-8 < y < 8$, and the window region includes five grid points. The figure shown above is the case where the window region is located at $0.48 < y < 0.56$, whose corresponding basic flow range is $0.4462 < c_r < 0.5080$. We can find a neutral wave inside this region for any wavenumber. The point where the phase speed is located at the centre of this window region is shown by the symbol $\times$.

4. The jump in the derivative across the constant potential vorticity window

We will examine in detail the features of the solutions constructed in the preceding section. Let ϕ_w be a solution whose phase speed is located inside the window region, i.e. the phase speed c satisfies $U(y_1) < c < U(y_2)$ where $y_1 < y < y_2$ is the small window region with $\mathrm{d}Q_w/\mathrm{d}y = 0$:

$$(U_w - c)\left(\frac{\mathrm{d}^2\phi_w}{\mathrm{d}y^2} - k^2\phi_w\right) + \frac{\mathrm{d}Q_w}{\mathrm{d}y}\phi_w = 0. \tag{4.1}$$

Although the solution ϕ_w of (4.1) is not extreme even around the critical point, its first derivative becomes large. We will estimate the jump in the first derivative $\mathrm{d}\phi_w/\mathrm{d}y$ on both sides of the critical point.

Let us consider a small region $y_a < y < y_b$, which includes the window region, i.e. y_a and y_b satisfy $y_a < y_1 < y_2 < y_b$. We will estimate the difference between $\mathrm{d}\phi_w/\mathrm{d}y$ at $y = y_a$ and that at $y = y_b$ in the limit of an infinitely small window or $y_1, y_2 \to y_c$. If (4.1) is divided by $U_w - c$ and integrated from $y_1 - 0$ to $y_1 + 0$, we obtain

$$\begin{aligned}\left[\frac{\mathrm{d}\phi_w}{\mathrm{d}y}\right]_{y_1-0}^{y_1+0} &= \int_{y_1-0}^{y_1+0}\left(k^2\phi_w - \frac{1}{U_w - c}\frac{\mathrm{d}Q_w}{\mathrm{d}y}\phi_w\right)\mathrm{d}y \\ &= -\frac{1}{U_w(y_1) - c}[Q_w]_{y_1-0}^{y_1+0}\phi_w(y_1) = -\frac{\overline{Q} - Q(y_1)}{U_w(y_1) - U_w(y_c)}\phi_w(y_1).\end{aligned} \tag{4.2}$$

https://doi.org/10.1017/jfm.2012.529 Published online by Cambridge University Press

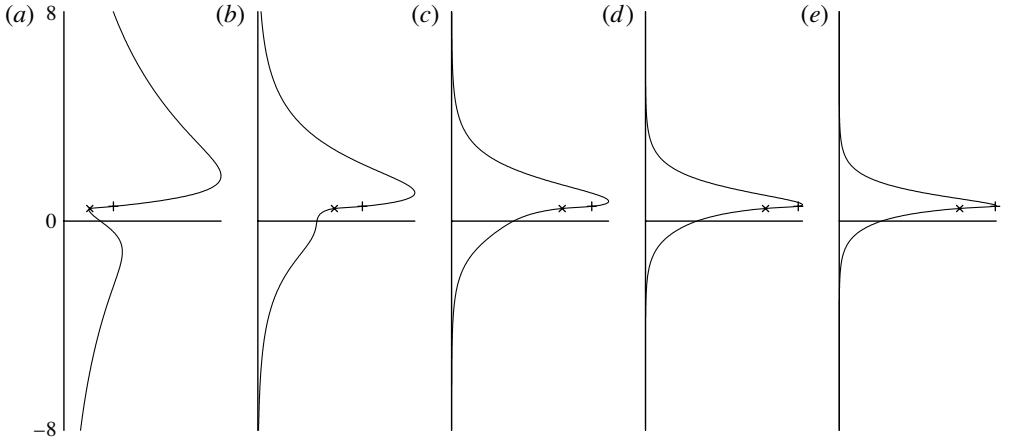


FIGURE 9. Structure of regular modes which appear inside the window region at (*a*) $k = 0.2$ ($c = 0.4496$), (*b*) $k = 0.6$ ($c = 0.4599$), (*c*) $k = 1.09$ ($c = 0.4772$), (*d*) $k = 1.6$ ($c = 0.4894$) and (*e*) $k = 2.0$ ($c = 0.4945$). The range between $y = 0.48$ indicated by symbols $\times$ and $y = 0.56$ by symbols $+$ corresponds to the window region. For $k = 0.2$ and 0.6, where the phase speed is close to $U = 0.4462$ or the basic flow velocity at the lower end of the window region $y = 0.48$, the velocity gradient has a large jump at $y = 0.48$, while for $k = 1.6$ and 2.0, where the phase speed is close to $U = 0.5080$ or the basic flow velocity at the upper end $y = 0.56$, it has a large jump at $y = 0.56$.

When we consider the limit $y_1, y_2 \to y_c$, we can estimate $\overline{Q} = (Q(y_1) + Q(y_2))/2$ in an infinitely small region, and thus we can calculate

$$\left[\frac{\mathrm{d}\phi_w}{\mathrm{d}y}\right]_{y_1-0}^{y_1+0} \to \frac{Q'(y_c)(y_2 - y_1)}{2U'(y_c)(y_c - y_1)}\phi_w(y_c) \quad \text{as } y_1, y_2 \to y_c. \tag{4.3}$$

On the other hand, as for the integration from y_a to $y_1 - 0$, since the contribution around $y \sim y_1$ becomes significant when $y_1 \to y_c$, we can estimate the major part of this integral as

$$\left[\frac{\mathrm{d}\phi_w}{\mathrm{d}y}\right]_{y_a}^{y_1-0} \to -\frac{Q'(y_c)}{U'(y_c)}\phi_w(y_c)\log(y_c - y_1) \quad \text{as } y_1 \to y_c. \tag{4.4}$$

In the same way, the change of $\mathrm{d}\phi_w/\mathrm{d}y$ around $y = y_2$ is estimated as

$$\left[\frac{\mathrm{d}\phi_w}{\mathrm{d}y}\right]_{y_2-0}^{y_2+0} \to -\frac{Q'(y_c)(y_2 - y_1)}{2U'(y_c)(y_2 - y_c)}\phi_w(y_c) \quad \text{as } y_1, y_2 \to y_c, \tag{4.5}$$

and

$$\left[\frac{\mathrm{d}\phi_w}{\mathrm{d}y}\right]_{y_2+0}^{y_b} \to \frac{Q'(y_c)}{U'(y_c)}\phi_w(y_c)\log(y_2 - y_c) \quad \text{as } y_2 \to y_c. \tag{4.6}$$

https://doi.org/10.1017/jfm.2012.529 Published online by Cambridge University Press

The jump beyond the window region in the limit of $y_1, y_2 \to y_c$ is calculated as their sum:

$$\left[\frac{\mathrm{d}\phi_w}{\mathrm{d}y}\right]_{y_a}^{y_b} = \left[\frac{\mathrm{d}\phi_w}{\mathrm{d}y}\right]_{y_a}^{y_1-0} + \left[\frac{\mathrm{d}\phi_w}{\mathrm{d}y}\right]_{y_1-0}^{y_1+0} + \left[\frac{\mathrm{d}\phi_w}{\mathrm{d}y}\right]_{y_2-0}^{y_2+0} + \left[\frac{\mathrm{d}\phi_w}{\mathrm{d}y}\right]_{y_2+0}^{y_b}$$
$$= \frac{Q'(y_c)}{U'(y_c)}\phi_w(y_c)\left[\frac{1-2r}{2r(1-r)} + \log\left(\frac{1-r}{r}\right)\right], \quad \text{where } r \equiv \frac{y_c - y_1}{y_2 - y_1}. \tag{4.7}$$

Using (4.7), we can explain as follows the feature described in the last section, that a regular mode always exists inside the small window region for any wavenumber. We can solve (4.1) in each region $y < y_1$, $y_1 < y < y_2$, and $y > y_2$, separately. If these solutions in three regions satisfy the continuity of ϕ_w and the connection conditions of $\mathrm{d}\phi_w/\mathrm{d}y$ (4.3) and (4.5), they construct an eigenfunction of the original problem. Here, the right-hand side of (4.7) can take any value by changing the value of r between 0 and 1. Therefore, we can always connect the solutions obtained in three regions only if we choose an adequate value of c between $U(y_1)$ and $U(y_2)$, which means that there always exists a solution.

However, when r is close to either 0 or 1, i.e. the phase speed is located close to either end of the window region, the sum of the jumps of the first derivative is very large, which indicates that the solution is largely modified around the window region. The condition that the sum of the jumps vanishes is realized when $r = 1/2$. The choice in the preceding section, of extracting a neutral mode located at the centre of the window region, corresponds to the choice of a mode the jumps of whose first derivative on both sides of the window region just cancel, since $r = 1/2$ is simply the case that the critical point is located at the centre of the window region.

5. Relation to continuous modes

For the original basic velocity profile without a window region, only continuous modes exist as modes with phase speed within the basic velocity range. Therefore, the neutral wave retrieved by opening a window region will approach some continuous mode when the width of the window region becomes infinitely small. A continuous mode whose phase speed c satisfies $c = U(y_c)$ can be expressed as a linear combination of three fundamental solutions:

$$\phi_{\mathrm{I}} = (y - y_c)\left[1 + \sum_{n=1}^{\infty} A_n (y - y_c)^n\right], \tag{5.1}$$

$$\phi_{\mathrm{II}r} = 1 + \sum_{n=1}^{\infty} B_n (y - y_c)^n - \frac{Q'(y_c)}{U'(y_c)}\phi_{\mathrm{I}} \log|y - y_c|, \tag{5.2}$$

$$\phi_{\mathrm{II}i} = \begin{cases} \pi\dfrac{Q'(y_c)}{U'(y_c)}\phi_{\mathrm{I}} & (y < y_c), \\ 0 & (y > y_c), \end{cases} \tag{5.3}$$

or

$$\phi_c(y) = C_{\mathrm{I}}\phi_{\mathrm{I}}(y) + C_{\mathrm{II}r}\phi_{\mathrm{II}r}(y) + C_{\mathrm{II}i}\phi_{\mathrm{II}i}(y) \tag{5.4}$$

(Lin 1961). While ϕ_{I} is regular, $\phi_{\mathrm{II}r}$ has a singularity of $(y - y_c)\log|y - y_c|$ at $y = y_c$, and $\phi_{\mathrm{II}i}$ has a singularity in that its first derivative is discontinuous at $y = y_c$ (figure 10).

https://doi.org/10.1017/jfm.2012.529 Published online by Cambridge University Press

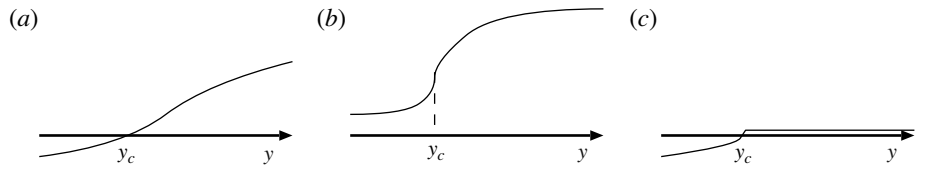


FIGURE 10. Three independent solutions forming a continuous mode: (*a*) ϕ_{I}; (*b*) $\phi_{\mathrm{II}r}$; (*c*) $\phi_{\mathrm{II}i}$. While ϕ_{I} is a regular solution, $\phi_{\mathrm{II}r}$ has a singularity of $(y-y_c)\log|y-y_c|$ at $y=y_c$, and $\phi_{\mathrm{II}i}$ has a singularity in that its first derivative is discontinuous at $y=y_c$.

For the solution ϕ_w obtained in § 3, the difference of $\mathrm{d}\phi_w/\mathrm{d}y$ beyond the window region vanishes in the limit of $y_2 \to y_1$, as examined in § 4. Therefore, the first derivative of the corresponding continuous mode in this limit should have no jump beyond the critical point y_c. Since $\phi_{\mathrm{I}}(y)$ is a regular solution, it naturally has no jump. For $\phi_{\mathrm{II}r}(y)$, while the sum of the jump is calculated using

$$\left[\frac{\mathrm{d}\phi_{\mathrm{II}r}}{\mathrm{d}y}\right]_{y_1-0}^{y_2+0} = -\frac{Q'(y_c)}{U'(y_c)}\phi_{\mathrm{I}}(y_c)\log\left(\frac{y_2-y_c}{y_c-y_1}\right), \tag{5.5}$$

it also vanishes, since we choose $(y_2-y_c)/(y_c-y_1) = (1-r)/r = 1$. Only $\phi_{\mathrm{II}i}(y)$ has a non-zero jump:

$$\left[\frac{\mathrm{d}\phi_{\mathrm{II}i}}{\mathrm{d}y}\right]_{y_1-0}^{y_2+0} = -\pi\frac{Q'(y_c)}{U'(y_c)}\phi_{\mathrm{I}}(y_c). \tag{5.6}$$

Therefore a continuous mode which satisfies the no-jump condition must not have non-zero coefficient $C_{\mathrm{II}i}$, or it would be expressed as

$$\phi_q(y) = C_{\mathrm{I}}\phi_{\mathrm{I}}(y) + C_{\mathrm{II}r}\phi_{\mathrm{II}r}(y). \tag{5.7}$$

We can see that the neutral wave derived by the method in § 3 corresponds to a continuous mode in the unmodified original basic state which does not have a jump singularity in its derivative as $\phi_{\mathrm{II}i}$, although it may have a singularity of the form $(y-y_c)\log|y-y_c|$ as $\phi_{\mathrm{II}r}$.

6. Numerical calculations

We obtained the dispersion curve of the hidden neutral wave by applying the method proposed in § 3 to the instability problem of the tanh-shaped shear flow (figure 1*b*). In figure 11, the dispersion relation of the hidden neutral wave obtained by sweeping the basic flow range with the uniform potential vorticity window is shown by dots. As expected, we can see a pair of dispersion curves with $c>0$ and $c<0$ at $k>1$, which leads to the unstable mode at $0<k<1$; it suggests that this shear instability can be understood by resonance between neutral waves.

In figure 11, the phase speed of continuous modes whose component of $\phi_{\mathrm{II}i}$ vanishes is also shown by dashed lines. In § 5, we showed that the method for retrieving a mode located in the centre of a window region is equivalent to the choice of a continuous mode without a singularity of $\phi_{\mathrm{II}i}$; the two different methods certainly derived almost the same dispersion curves.

In order to show more clearly that the shear instability can be understood by resonance between neutral waves, we show in figure 12 the eigenfunctions of the

https://doi.org/10.1017/jfm.2012.529 Published online by Cambridge University Press

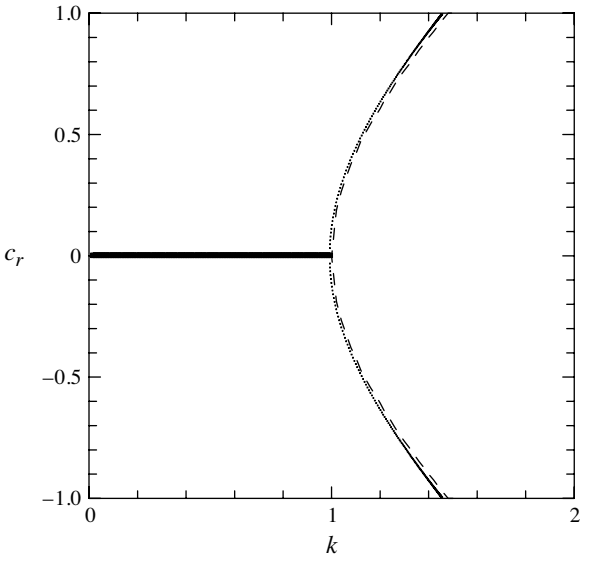


FIGURE 11. Dispersion curves of hidden neutral waves retrieved by the method proposed in this article. For the numerical calculation, 1000 grid points are placed in the region $-8 < y < 8$. Dots indicate neutral waves retrieved by making a small window region with uniform potential vorticity (which includes five grid points or a width of $\Delta y = 0.08$) and sweeping the basic flow range, which appear in the wavenumber region $1 < k \lesssim 1.47$ as two modes leading to the unstable mode at $0 < k < 1$ (shown by a thick line). The dashed lines indicate continuous modes without singularities in $\phi_{\mathrm{III}i}$, which are obtained by the criterion that the difference for $\mathrm{d}\phi/\mathrm{d}y|_{y=y_c}$, calculated on both sides of $y = y_c$, vanishes on extrapolation.

unstable mode and the retrieved neutral waves. The retrieved neutral waves have a large amplitude around $y = 1$ and $y = -1$, respectively. The structure of the unstable mode is very similar to the superposition of these neutral waves elongated and shifted in the x-direction, and this correspondence shows that the unstable mode is well explained by resonance between the neutral waves.

The features of the dispersion curves of the retrieved neutral waves (figure 11) and the structures of the eigenfunction of the unstable and neutral modes (figure 12) are very similar to those for the piecewise linear basic velocity profile, where we can easily find dispersion curves of neutral waves connecting to the unstable modes (figures 2 and 4).

The shear instability in the piecewise linear basic flow is interpreted by resonance between a pair of vorticity waves, one of which is caused by a positive potential vorticity gradient in $y > 0$ and the other is caused by a negative gradient in $y < 0$. Therefore, it is plausible to assume that retrieved neutral waves have similar physical properties by analogy. As we can see in figure 12(*b*), the point where the amplitude of the retrieved wave with positive phase speed becomes maximum (y_m) is slightly shifted in the positive direction from the critical point ($y_m > y_c$). The potential vorticity gradient is positive in a wide region including y_m, which can cause a vorticity wave. Since $U(y)$ increases monotonically in this situation, the relation $y_m > y_c$ means $c < U(y_m)$. Since the phase speed of this wave is smaller than the basic flow velocity at the maximum-amplitude point, this wave propagates intrinsically in the negative

https://doi.org/10.1017/jfm.2012.529 Published online by Cambridge University Press

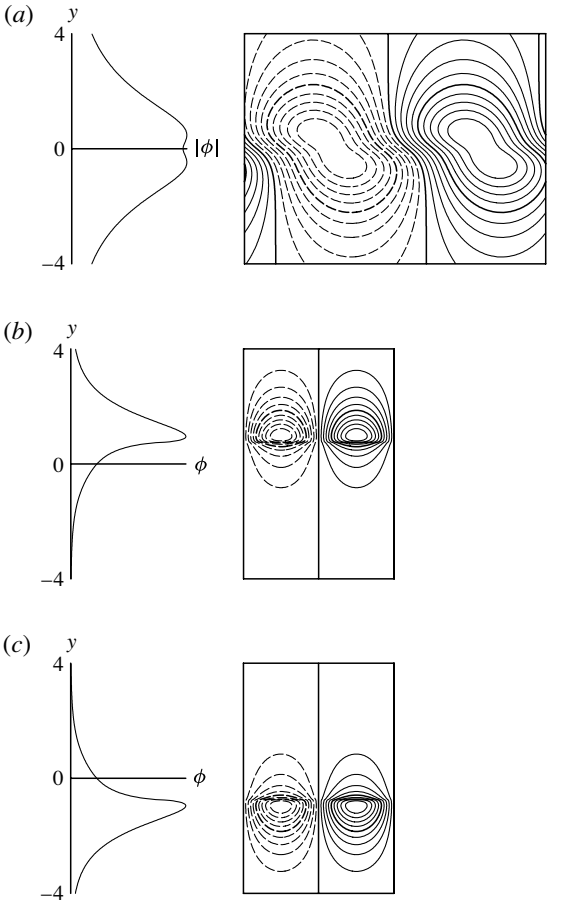


FIGURE 12. (*a*) The unstable mode at $k = 0.6$ ($c = 0.2883\mathrm{i}$). (*b*) The retrieved neutral wave with positive phase speed $c = 0.6315 > 0$ at $k = 1.2$. (*c*) The retrieved neutral wave with negative phase speed $c = -0.6315 < 0$ at $k = 1.2$. The eigenfunction ϕ of each mode is shown. The retrieved neutral waves have an amplitude peak around $y = 1$ and $y = -1$, respectively. The structure of the unstable mode is very similar to the superposition of structures of the two neutral waves elongated and shifted in the x-direction; it also shows that the unstable mode can be explained by resonance between these neutral waves.

direction, which is consistent with the feature of vorticity waves in a basic flow with a positive potential vorticity gradient.

There are also some features different to those in the case with a piecewise linear basic velocity profile: one of the most distinct differences is that the dispersion curves of the retrieved neutral waves do not extend to $k \to \infty$ but reach the limit of the basic flow range $c = \pm 1$ within finite k. Figure 11 indicates the value as $k \sim 1.47$. In the following, we will consider this behaviour of the retrieved dispersion curves.

Since $y_c \to \pm\infty$ as $c \to \pm 1$, this limit corresponds to the case when the critical point is located far from the shear zone. The region where the neutral wave has a substantial amplitude is considered to be concentrated around the critical point. Thus, by approximating the term $U - c$ linearly around $y = y_c$, and by representing $\mathrm{d}Q/\mathrm{d}y$

https://doi.org/10.1017/jfm.2012.529 Published online by Cambridge University Press

with its value at $y = y_c$, we can approximate (2.4) as

$$\frac{\mathrm{d}^2\phi}{\mathrm{d}y^2} - k^2\phi + \frac{Q'(y_c)}{U'(y_c)(y - y_c)}\phi = 0. \tag{6.1}$$

This means that the problem is reduced to the simplest situation: a problem of retrieving neutral waves in a uniform shear with uniform potential vorticity gradient. In this case, the wavenumber is obtained as $k = 1.0000 \times [Q'(y_c)/U'(y_c)]$ (see the Appendix). Since we are considering $U = \tanh y$, and thus $\mathrm{d}U/\mathrm{d}y = \mathrm{sech}^2 y$ and $\mathrm{d}Q/\mathrm{d}y = -\mathrm{d}^2U/\mathrm{d}y^2 = 2\mathrm{sech}^2 y \tanh y$, the ratio of Q' to U' becomes

$$\frac{Q'(y_c)}{U'(y_c)} = \frac{2\mathrm{sech}^2 y_c \tanh y_c}{\mathrm{sech}^2 y_c} = 2\tanh y_c \to 2 \quad \text{as } y_c \to +\infty, \tag{6.2}$$

and we can estimate the wavenumber as $k \sim 2.0000$.

Since Q'/U' converges to a finite value at infinity in the case of tanh-shaped shear flow, we can explain that the wavenumber k remains finite in the limit of $c \to \pm 1$ or the boundary of the area where the basic flow exists, but the derived value of the wavenumber is larger than that shown in the dispersion curve. In the case of a basic flow with uniform shear and potential vorticity gradient, the amplitude of the derived neutral wave decays as $\phi \sim \exp(\mp ky)$ far from the critical point. However, in the case of tanh-shaped shear flow, the amplitude of the derived neutral wave, whose critical point is located far from the shear zone ($y_c \gg 1$), decays as $\phi \sim \exp(-ky)$ at $y \gg y_c$ (at the positive far side), but it decays as $\phi \sim \exp(\sqrt{k^2 + 4}y)$ at $y_c \gg y \gg 1$ (at the negative far side but at the positive far side from the shear zone). This may affect the estimation of the value of k. In order to give a better estimation, we need more accurate approximation of the basic flow. Since

$$\begin{aligned}\frac{\mathrm{d}Q/\mathrm{d}y}{U - c} &= \frac{2\mathrm{sech}^2 y \tanh y}{\tanh y - \tanh y_c} \\ &\sim \frac{8\mathrm{e}^{-2y}}{(1 - 2\mathrm{e}^{-2y}) - (1 - 2\mathrm{e}^{-2y_c})} = \frac{4}{\mathrm{e}^{2(y - y_c)} - 1} = 2\left[\coth(y - y_c) - 1\right],\end{aligned} \tag{6.3}$$

for large y and y_c, (2.4) is approximated by

$$\frac{\mathrm{d}^2\phi}{\mathrm{d}y^2} - k^2\phi + 2\left[\coth(y - y_c) - 1\right]\phi = 0. \tag{6.4}$$

We obtain from this approximated equation the value $k \sim 1.4996$ (see the Appendix); this value is close to that shown in the dispersion curve.

7. Comparison with the broken-line velocity profile case

In previous sections we discussed how to retrieve neutral waves connected to the unstable mode for the tanh-shaped velocity profile basic state. When we examine the instability of such flows, in general, we often approximate the velocity profile by broken straight lines connecting discrete representative points. Once we a consider velocity profile consisting of broken straight lines, we are free from the mathematical difficulty that no regular neutral mode can exist, since its potential vorticity is piecewise uniform. Tatsumi *et al.* (1964) considered a basic flow profile made up of straight lines connecting $U(y_i)$ or velocity at discrete points $y_i (i = 1, \ldots, N)$ of a tanh-shaped profile, and obtained its dispersion curves. They showed that the dispersion curves connected to the unstable mode behave as $c_r \sim 0$ in the limit of $k \to \infty$,

https://doi.org/10.1017/jfm.2012.529 Published online by Cambridge University Press

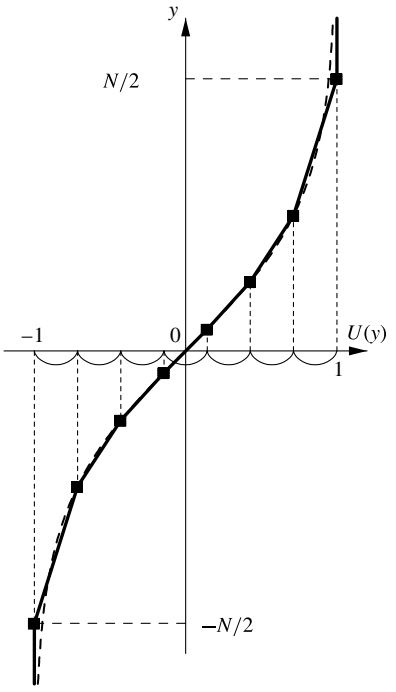


FIGURE 13. Velocity profile of the basic flow approximated by broken straight lines.

since dispersion curves of neutral waves only shift from $U(y_i)$ to $U(y_{i+1})$; superficially, this feature seems to contradict our results in this article. In this section, we will examine the consistency between the behaviour of neutral waves in the case of a broken-line velocity profile and the results shown in previous sections. First, we solve the dispersion curves for the basic state of a broken-line velocity profile: we consider the basic velocity profile (figure 13) of

$$U(y) = \begin{cases} -1, & (y < y_1), \\ \dfrac{U_{j+1} - U_j}{y_{j+1} - y_j}(y - y_j) + U_j, & (y_j < y < y_{j+1},\ j = 1, \ldots, N-1), \\ 1, & (y > y_N), \end{cases} \tag{7.1}$$

where

$$\left.\begin{array}{ll} U_1 = -1, & y_1 = -\dfrac{N}{2}, \\ U_j = -1 + \dfrac{2(j-1)}{N-1}, & y_j = \dfrac{1}{2}\log\left(\dfrac{1+U_j}{1-U_j}\right), \quad (j = 2, \ldots, N-1) \\ U_N = 1, & y_N = \dfrac{N}{2}. \end{array}\right\} \tag{7.2}$$

In figure 14 we show dispersion curves obtained for several values of N. The dispersion curves connected to the unstable mode around $k = 1$ really behave as $c \to U_{(N/2)}, U_{(N/2)+1}$ in the limit of $k \to \infty$; they approach 0 when N becomes large. However, it does not indicate that the two resonating neutral waves causing the

https://doi.org/10.1017/jfm.2012.529 Published online by Cambridge University Press

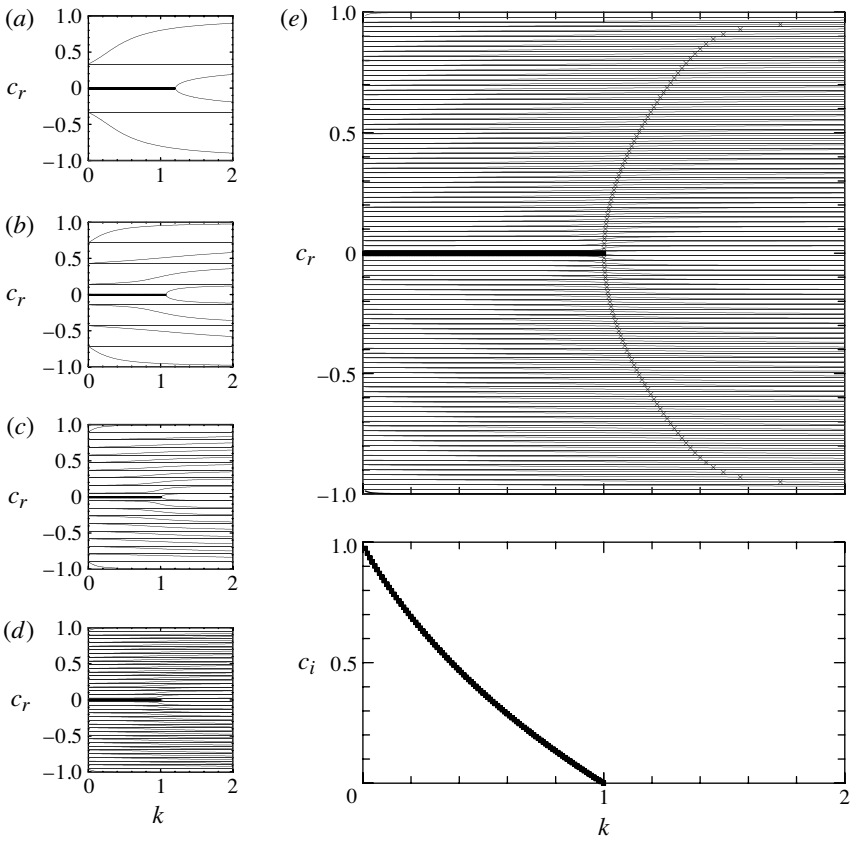


FIGURE 14. Dispersion curves for the basic flow whose velocity profile is approximated by $N + 1$ broken straight lines: (*a*) $N = 4$; (*b*) $N = 8$; (*c*) $N = 20$; (*d*) $N = 40$; (*e*) $N = 100$. An unstable mode is indicated by a thick line. The basic velocity at each edge of the broken-line velocity profile is shown by thin lines. Each dispersion curve approaches the basic velocity at one of the velocity profile edges in the limits of $k \to 0$ and ∞. In the figure for $N = 100$ (*e*), the symbols $\times$ indicate the points where dispersion curves shift half the distance of the phase speed gap between two neighbouring modes.

unstable mode are the two modes with $c \sim 0$, considering that waves with similar features are not necessarily expressed by a single dispersion curve, as discussed below.

Let us consider two dispersion curves with phase speeds close together, whose pseudomomenta have the same sign. They exist independently when not interacting (figure 15*a*, *b*). When they coexist and mutually interact they do not cause instability since their pseudomomenta have the same sign, but their dispersion curves 'interchange' (figure 15*c*). In figure 15(*c*), mode [A] at a small wavenumber should be identified not as mode [B], which is on the same dispersion curve, but as mode [C]; although [B] is connected to [A] by one dispersion curve, it is physically different from [A] considering its origin. Further, let us consider that one counterpart of the interacting pair is not a single mode, but a bundle of many neutral waves with phase speeds close together (figure 15*d*). In this case, the interchanges occur successively, and each dispersion curve in the bundle shifts from a phase speed of one mode to that of the next one (figure 15*e*). Also in this case of figure 15(*e*), the mode [D] at small

https://doi.org/10.1017/jfm.2012.529 Published online by Cambridge University Press

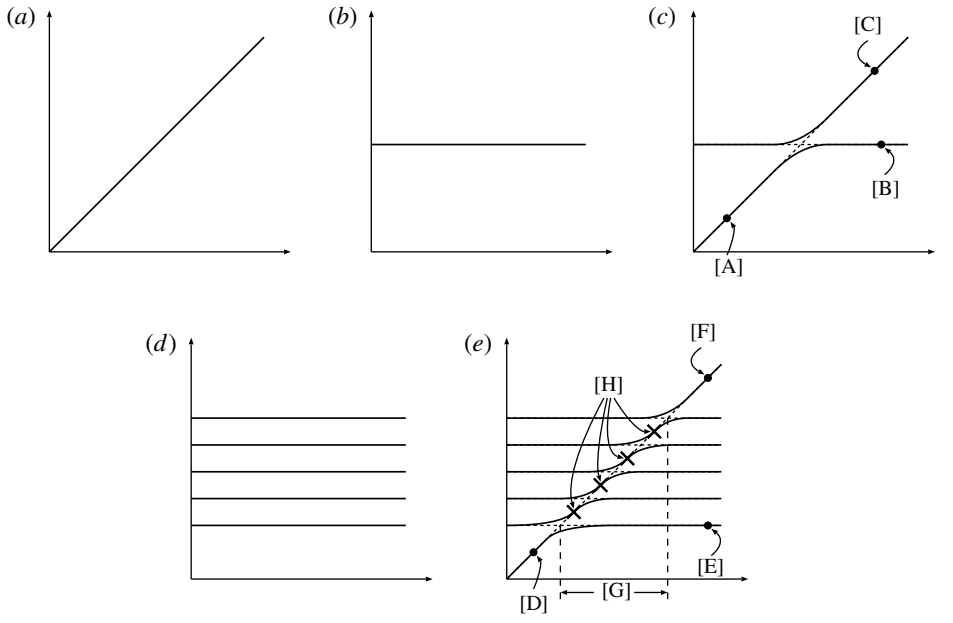


FIGURE 15. (*a*) A dispersion curve of a certain neutral wave, without interaction with other modes. (*b*) A dispersion curve of another neutral wave, without interaction with other modes. (*c*) Dispersion curves where mode (*a*) and mode (*b*) coexist and weakly interact. (*d*) Dispersion curves of a bundle of neutral waves other than mode (*a*), without interaction with other modes. (*e*) Dispersion curves where mode (*a*) and modes (*d*) coexist and weakly interact.

wavenumbers should be identified not as mode [E], which is on the same dispersion curve, but as mode [F].

Concluding that the pair of neutral modes causing the unstable mode is the pair of close modes with $c \sim 0$ from the dispersion curves for the broken-line velocity profile case is equivalent to identifying mode [E] as mode [D].

Although we can consider [F] as corresponding to [D] in large wavenumbers, it is not simple to identify the correspondence of [D] in the wavenumber region where interchanges are successively occurring ([G] in figure 15*e*). Nevertheless, in this case too, we can show it by picking up the points where the dispersion curves shift half the distance of the phase speed gap between two neighbouring modes, as indicated by [H] in figure 15(*e*).

Let us review figure 14 from this standpoint. The symbols $\times$ in the case of $N = 100$ (figure 14*e*) indicate the points where the dispersion curves shift half the distance or where the phase speed becomes $c = (U_j + U_{j+1})/2$. The points indicated by symbols $\times$ form almost the same curve as figure 11 except at $c \sim \pm 1$, which corresponds to the region where the edges of the broken lines are sparsely distributed. This result confirms that we can consider that two neutral modes identical to that obtained from the discussions in the previous sections initially exist in the broken-line velocity profile case too, but they are interchanged successively with many neutral waves caused by edges of the approximated basic velocity profile.

The case where the interacting counterpart is the bundle of continuous modes instead of many regular neutral modes has been shown by Iga (1999*a*) (see his

https://doi.org/10.1017/jfm.2012.529 Published online by Cambridge University Press

figure 6*b*). We take the view that the method for retrieving neutral modes hidden in shear flow discussed in the previous sections in this article is simply the method for retrieving neutral modes interchanged with continuous modes.

8. Conclusions

In order to apply the understanding of instability via resonance between neutral waves to shear instability in a basic flow with non-uniform potential vorticity such as a tanh-shaped velocity profile, we proposed a method for retrieving neutral waves hidden in the shear of the basic flow. When the basic flow has a shear, except for the special case when the potential vorticity gradient just vanishes, no neutral wave with a critical point exists. Even in cases where a wave is expected to exist from physical considerations, a mode does not exist mathematically in general, owing to this constraint. However, we took the view that it is because a neutral wave is hidden in the shear, and showed a method for retrieving it: we modify a small part of the basic flow to make its potential vorticity uniform, keeping most other parts unchanged, investigate the neutral wave which appears in this window region where neutral waves can exist, and retrieve the whole dispersion curve by sweeping the basic flow range.

The neutral wave which appears in the window region is strongly modified when its phase speed is close to one end of the region. Thus, we selected a neutral wave located at the centre of the window region. This corresponds to the choice of a solution whose jump in the first derivative at one end of the window region cancels that at the other end. It is also equivalent to a choice of a continuous mode which does not have a jump in its first derivative at the critical point even if it can have a singularity of $(y - y_c)\log|y - y_c|$, in the limit that the width of the window region is infinitely small.

It is shown that the structure of the unstable mode in a tanh-shaped shear flow is similar to the superposition of neutral waves hidden in the shear with non-zero potential vorticity gradient, which are retrieved in this way, elongated and shifted in the x-direction. Application of this method also enables us to understand instability in a shear flow with non-uniform potential vorticity, to which it was difficult to apply the explanation by the physical concept of resonance between neutral waves, since neutral waves leading to the unstable mode are not found.

In this paper, we have shown that shear instability can be understood as a resonance between neutral waves hidden in the background flow. The proposed method can also be used to analyse neutral modes in parallel shear flows.

Acknowledgements

The LAPACK Library was used to solve the eigenvalue problem and the NCARG Library was used to draw some figures.

Appendix. Solutions of approximated basic situations

As the simplest situation, where neutral waves are hidden in the shear and thus the method proposed in this article should be applied, we can consider a problem of obtaining neutral waves in a shear flow with non-zero uniform shear ($U' = \text{const.} \neq 0$) and non-zero uniform potential vorticity ($Q' = \text{const.} \neq 0$). We can realize such a situation by considering a linear basic flow ($U(y) = ay + b$) on a beta plane ($\beta \neq 0$):

$$\frac{\mathrm{d}^2\phi}{\mathrm{d}y^2} - k^2\phi + \frac{Q'}{U'(y - y_c)}\phi = 0. \tag{A 1}$$

https://doi.org/10.1017/jfm.2012.529 Published online by Cambridge University Press

By shifting in the y-direction and non-dimensionalizing as $y_* \equiv (Q'/U')(y - y_c)$, $k_* \equiv (U'/Q')k$, (A 1) becomes

$$\frac{\mathrm{d}^2\phi}{\mathrm{d}y_*^2} - k_*^2\phi + \frac{1}{y_*}\phi = 0. \tag{A 2}$$

Further, this equation becomes

$$\frac{\mathrm{d}\psi}{\mathrm{d}y_*} + \psi^2 - k_*^2 + \frac{1}{y_*} = 0, \tag{A 3}$$

for ψ defined by $\psi \equiv (\mathrm{d}\phi/\mathrm{d}y_*)/\phi$. Since the third term of the left-hand side of (A 2) becomes small at $y_* \to \pm\infty$, we can consider $\phi \sim \exp(\mp k_* y_*)$ as $y_* \to \pm\infty$. On the other hand, from the behaviour of the solution considered here around the singularity, we have $\mathrm{d}\phi/\mathrm{d}y_*|_{y_*=+\epsilon} - \mathrm{d}\phi/\mathrm{d}y_*|_{y_*=-\epsilon} \to 0$ as $\epsilon \to +0$. These give boundary conditions for ψ as

$$\begin{cases} \psi \to -k & \text{as } y_* \to +\infty, \\ \psi \to k & \text{as } y_* \to -\infty, \\ \psi(+\epsilon) - \psi(-\epsilon) \to 0 & \text{as } \epsilon \to +0. \end{cases} \tag{A 4}$$

Defining functions ψ_+ and ψ_- at $y_* > 0$ as $\psi_+ \equiv \psi(y_*) + \psi(-y_*)$ and $\psi_- \equiv \psi(y_*) - \psi(-y_*) + 2k_*$, (A 3) and (A 4) become

$$\frac{\mathrm{d}\psi_+}{\mathrm{d}y_*} - 2k_*\psi_+ + \psi_+ \cdot \psi_- + \frac{2}{y_*} = 0, \tag{A 5}$$

$$\frac{\mathrm{d}\psi_-}{\mathrm{d}y_*} + \frac{1}{2}\psi_+^2 + \frac{1}{2}\psi_-^2 - 2k_*\psi_- = 0, \tag{A 6}$$

$$\begin{cases} \psi_+ \to 0 & \text{as } y_* \to +\infty, \\ \psi_- \to 0 & \text{as } y_* \to +\infty, \\ \psi_- \to 2k_* & \text{as } y_* \to +0. \end{cases} \tag{A 7}$$

For large y_*, we may expect $|\psi_-| \ll k_*$ since ψ_- approaches zero. For small y_*, on the other hand, we may expect $|\psi_-| \ll 1/y_*$ and $|\psi_-| \ll |\psi_+|$ since $1/y_*$ and ψ_+ diverges to infinity. Thus we can approximate (A 5) and (A 6) as

$$\frac{\mathrm{d}\psi_+}{\mathrm{d}y_*} - 2k_*\psi_+ + \frac{2}{y_*} = 0, \tag{A 8}$$

$$\frac{\mathrm{d}\psi_-}{\mathrm{d}y_*} + \frac{1}{2}\psi_+^2 - 2k_*\psi_- = 0. \tag{A 9}$$

From (A 8), we can obtain ψ_+ for the approximated equations using

$$\psi_+(y_*) = \mathrm{e}^{2k_*y_*}\int_{y_*}^{\infty} \frac{2\mathrm{e}^{-2k_*y'}}{y'}\,\mathrm{d}y' = -2\mathrm{e}^{2k_*y_*}\mathrm{Ei}(-2k_*y_*), \tag{A 10}$$

where Ei is the integral exponential function defined by

$$\mathrm{Ei}(-x) \equiv -\int_x^{\infty} \frac{\mathrm{e}^{-t}}{t}\,\mathrm{d}t. \tag{A 11}$$

https://doi.org/10.1017/jfm.2012.529 Published online by Cambridge University Press

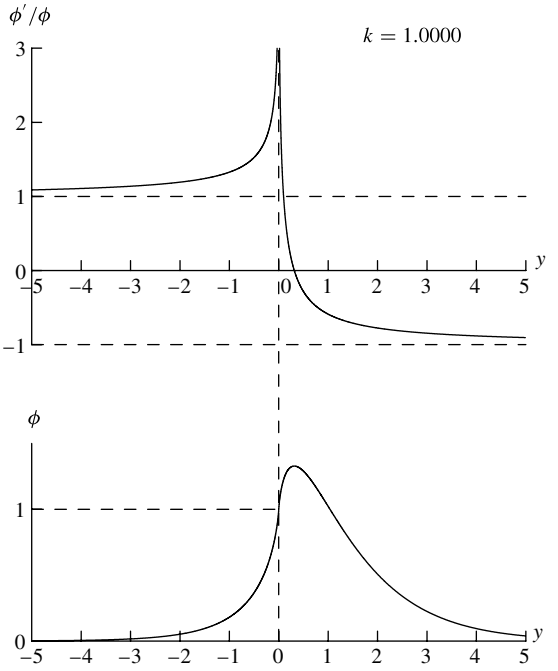


FIGURE 16. Solution of (A 2) for ϕ and (A 3) for $\psi = \phi'/\phi$, $k = 1.0$.

By substituting the obtained ψ_+ into (A 9), we obtain the approximate solution ψ_- as

$$\psi_-(y_*) = \mathrm{e}^{2k_* y_*} \int_{y_*}^{\infty} \mathrm{e}^{-2k_* y'} \frac{\psi_+^2(y')}{2}\,\mathrm{d}y' = 2\mathrm{e}^{2k_* y_*} \int_{y_*}^{\infty} \mathrm{e}^{2k_* y'} \mathrm{Ei}^2(-2k_* y')\,\mathrm{d}y'. \quad \text{(A 12)}$$

The value of ψ_- in the limit of $y_* \to 0$ is calculated to be

$$\psi_-(0) = 2\int_0^{\infty} \mathrm{e}^{2k_* y'} \mathrm{Ei}^2(-2k_* y')\,\mathrm{d}y' = \frac{1}{k_*}\int_0^{\infty} \mathrm{e}^{y} \mathrm{Ei}^2(-y)\,\mathrm{d}y, \quad \text{(A 13)}$$

which should be equal to $2k_*$, from the boundary condition. Therefore, we obtain k_* as

$$k_* = \left[\frac{1}{2}\int_0^{\infty} \mathrm{e}^{y} \mathrm{Ei}^2(-y)\,\mathrm{d}y\right]^{1/2} \sim 0.9069. \quad \text{(A 14)}$$

In order to solve the original exact equations (A 5) and (A 6), we use an iterative method substituting the approximated values as the omitted nonlinear terms and k_*. The functions ψ and ϕ are shown in figure 16 and we obtain the value of k_* as

$$k_* \sim 1.0000, \quad \text{(A 15)}$$

or

$$k \sim 1.0000 \times (Q'/U') \quad \text{(A 16)}$$

in dimensional units.

https://doi.org/10.1017/jfm.2012.529 Published online by Cambridge University Press

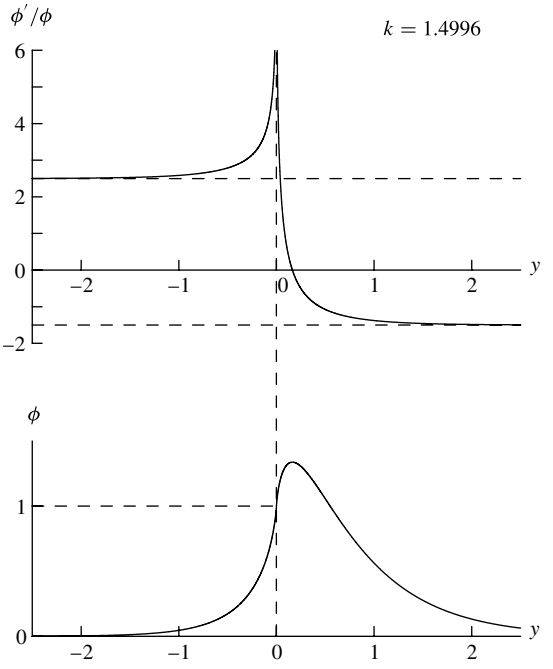


FIGURE 17. Solution of (A 17) for ϕ and (A 18) for $\psi = \phi'/\phi$, $k = 1.4996$.

The equation (6.4) is also modified to

$$\frac{\mathrm{d}^2\phi}{\mathrm{d}y_*^2} - k^2\phi + 2\,(\coth y_* - 1)\,\phi = 0, \tag{A 17}$$

by shifting in the y-direction as $y_* \equiv y - y_c$, or the equation for $\psi \equiv (\mathrm{d}\phi/\mathrm{d}y_*)/\phi$ is

$$\frac{\mathrm{d}\psi}{\mathrm{d}y_*} + \psi^2 - k^2 + 2\,(\coth y_* - 1) = 0. \tag{A 18}$$

We can obtain the solution using iteration. The functions ψ and ϕ are shown in figure 17 and we obtain the value of k as

$$k \sim 1.4996. \tag{A 19}$$

REFERENCES

BAINES, P. G. & MITSUDERA, H. 1994 On the mechanism of shear flow instabilities. *J. Fluid Mech.* **276**, 327–342.

BRETHERTON, F. P. 1966 Critical layer instability in baroclinic flows. *Q. J. Roy. Meteorol. Soc.* **92**, 325–334.

CAIRNS, R. A. 1979 The role of negative energy waves in some instabilities of parallel flows. *J. Fluid Mech.* **92**, 1–14.

CASE, K. M. 1960 Stability of inviscid plane Couette flow. *Phys. Fluids* **3**, 143–148.

DRAZIN, P. & REID, W. 1981 *Hydrodynamic Stability*. Cambridge University Press.

GOTOH, K. 1965 The damping of the large wavenumber disturbances in a free boundary layer flow. *J. Phys. Soc. Japan* **20**, 164–169.

https://doi.org/10.1017/jfm.2012.529 Published online by Cambridge University Press

HAYASHI, Y.-Y. & YOUNG, W. R. 1987 Stable and unstable shear modes on rotating parallel flows in shallow water. *J. Fluid Mech.* **184**, 477–504.

IGA, K. 1993 Reconsideration of Orlanski's instability theory of frontal waves. *J. Fluid Mech.* **255**, 213–236.

IGA, K. 1997 Instability of a front with a layer of uniform potential vorticity. *J. Met. Soc. Japan* **75**, 1–11.

IGA, K. 1999*a* Critical layer instability as a resonance between a non-singular mode and continuous modes. *Fluid Dyn. Res.* **25**, 63–86.

IGA, K. 1999*b* A simple criterion for the sign of the pseudomomentum of modes in shallow water systems. *J. Fluid Mech.* **387**, 343–352.

IGA, K. & IKAZAKI, H. 2000 Instability of a front formed by two layers with uniform potential vorticity. *J. Met. Soc. Japan* **78**, 491–498.

LIN, C. C. 1945 On the stability of two-dimensional parallel flows. Part 2. *Q. Appl. Math.* **3**, 218–234.

LIN, C. C. 1961 Some mathematical problems in the theory of the stability of parallel flows. *J. Fluid Mech.* **10**, 430–438.

MICHALKE, A. 1964 On the inviscid instability of the hyperbolic-tangent velocity profile. *J. Fluid Mech.* **19**, 543–556.

SAKAI, S. 1989 Rossby–Kelvin instability: a new type of ageostrophic instability caused by a resonance between Rossby waves and gravity waves. *J. Fluid Mech.* **202**, 149–176.

TANIGUCHI, H. & ISHIWATARI, M. 2006 Physical interpretation of unstable modes of a linear shear flow in shallow water on an equatorial beta-plane. *J. Fluid Mech.* **567**, 1–26.

TATSUMI, T, GOTOH, K. & AYUKAWA, K. 1964 The stability of a free boundary layer at large Reynolds numbers. *J. Phys. Soc. Japan* **19**, 1966–1980.

VALLIS, G. K. 2006 *Atmospheric and Oceanic Fluid Dynamics*. Cambridge University Press.

https://doi.org/10.1017/jfm.2012.529 Published online by Cambridge University Press